Limited Regional Aerosol Changes Despite Unprecedented Decline in Nitrogen Oxide Pollution During the February 2020 Coronavirus Shutdown in China

Michael S. Diamond & Robert Wood

Department of Atmospheric Sciences, University of Washington, Seattle, USA

Corresponding author: Michael Diamond (diamond2@uw.edu)

Key Points:

- Rapid economic collapse in February 2020 due to the COVID-19 pandemic and partial recovery in March 2020 unique in recent Chinese history
- Regional decline in NO_x pollution is unprecedented in the satellite record, but no change in aerosol or cloud properties is observed
- Differential economic impacts by sector, with transportation hit particularly hard, may explain differences in NO_x and aerosol response

Abstract

Following the emergence of a novel coronavirus in Wuhan, the People's Republic of China instituted a number of strict lockdown and more general socio-economic shutdown measures throughout the country starting in late January and continuing into February 2020 in order to arrest the spread of the disease. This resulted in a sharp economic contraction unparalleled in recent Chinese history. Satellite remote sensing shows that nitrogen oxide pollution declined by an unprecedented amount (~50% regionally) from its expected unperturbed value, but regional-scale column aerosol loadings and cloud microphysical properties were not detectably affected. The disparate impact may be tied to differential economic impacts of the shutdown, in which the transportation sector, a disproportionate source of nitrogen oxide emissions, underwent drastic declines (~90% reductions in passenger traffic), whereas industry and power generation, responsible for >90% of particulate emissions, were relatively less affected (~10% reductions in electricity and thermal power generation).

Plain Language Summary

To slow the spread of COVID-19, China put in place strict policies to limit travel and public gatherings in February 2020, resulting in a pronounced decline in the economy. Satellite measurements show that levels of nitrogen oxides, gases that are a major component of air pollution, were substantially lower than what we would normally expect for February. Surprisingly, however, we did not observe any similar changes in airborne particles (another major component of air pollution) or in the size of cloud droplets (which is partly determined by how many airborne particles there are). This is important because airborne particles, in addition to harming human health, affect the climate by changing how much sunlight is absorbed on Earth versus reflected back into space. The transportation sector of the economy was hit particularly hard by the coronavirus shutdown, but heavy industries and power plants were relatively less affected. Transportation is a major source of nitrogen oxides but not airborne particles, which are mostly emitted by industry and power plants. The shutdown's much larger effect on transportation than on industry or power plants can therefore help to explain the differences we see in the different types of air pollution.

1 Introduction

1.1 Emergence of a Novel Coronavirus and the Societal Response to the Resulting COVID-19 Pandemic

In late December 2019, cases of a pneumonia of unknown cause were reported in the city of Wuhan. By January 2020, the pathogen responsible—discovered to be a novel zoonotic coronavirus—had already spread throughout China and other nations including Japan, South Korea, and the United States (C. Wang et al., 2020). To arrest the spread of COVID-19 (the disease caused by the novel coronavirus), a series of unprecedently strict restrictions on travel and other activities were adapted across China, slowing the spread of the epidemic in China even as the disease became a global pandemic (Maier & Brockmann, 2020; Tian et al., 2020).

Unsurprisingly, this socio-economic "shutdown" had a catastrophic effect on the Chinese economy. Figure 1 shows the Purchasing Managers' Index (PMI) for both manufacturing and non-manufacturing sectors as reported by the National Bureau of Statistics of China. The PMI is a survey-based estimate of economic activity, with values above 50% corresponding to growth and below to contraction (Harris, 1991). February 2020 stands out sharply, featuring a decline in manufacturing PMI deeper than any point during the aftermath of the 2008 financial crisis and the only period of contraction in non-manufacturing PMI since records for that index began in 2007, followed by a rapid recovery. In this paper, we analyze whether there were detectable environmental changes associated with this sharp February 2020 downturn.

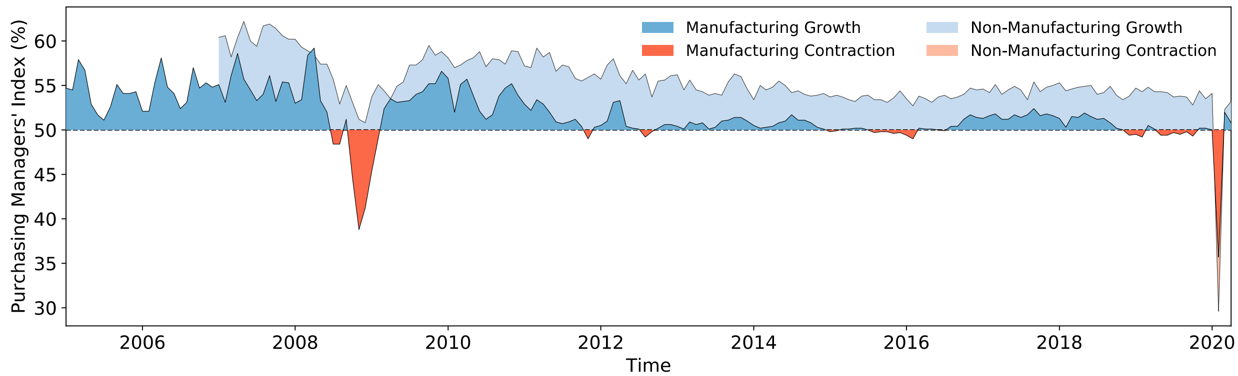

Figure 1. China's Purchasing Managers' Index from January 2005 to April 2020. Economic growth is indicated by blue shading and contraction by red shading (darker colors signify the manufacturing and lighter colors the non-manufacturing sectors).

1.2 Anthropogenic Drivers of Recent Pollution Changes

Nitrogen oxides ($NO_x \equiv NO + NO_2$) are reactive, short-lived gases that are a major constituent of air pollution harmful to human health (Atkinson et al., 2018). Due to rapid cycling between NO and NO_2 in the atmosphere, changes in NO_2 indicate changes in NO_x overall. Tiny particles suspended in the air (aerosol) are another major component of air pollution. Particulate matter with aerodynamic diameters of 2.5 μm or smaller (PM2.5) is known to have severe health impacts, with some estimates of global excess mortality due to outdoor PM2.5 approaching 10 million deaths annually (Burnett et al., 2018).

In addition to their relevance for public health, aerosol particles influence the climate through absorbing and scattering sunlight and by changing the optical properties of other components of the Earth system like snow, ice, and clouds. In particular, gaps in our knowledge about the interactions between clouds and aerosol particles represent the largest source of uncertainty in present-day anthropogenic radiative forcing in the most recent Intergovernmental Panel on Climate Change (IPCC) assessment (Myhre et al., 2013). Aerosol particles can serve as cloud condensation nuclei (CCN) upon which liquid-phase cloud droplets may form. Increasing CCN increases the number of cloud droplets and (for the same amount of liquid water) decreases their size, increasing cloud reflectivity (Twomey, 1977). Macrophysical cloud adjustments to these microphysical changes can either enhance or offset this "Twomey effect" (Ackerman et al., 2004; Albrecht, 1989). Aerosol also influence mixed-phase and ice cloud properties, although the climatic effects of these changes are even less certain (Storelvmo, 2017).

Determining whether observed cloud changes are attributable to aerosol or meteorological factors is a major challenge (Gryspeerdt et al., 2016; Stevens & Feingold, 2009). To better constrain causality, there has been a growing literature on “natural experiments” like volcanic eruptions and inadvertent anthropogenic modifications like ship tracks (Malavelle et al., 2017; Toll et al., 2019). A clear signal in aerosol and cloud properties due to the February 2020 shutdown would be of great interest to those working to constrain the magnitude of aerosol-cloud interactions (ACI), especially over land.

Both long-term changes in air pollution and ACI over China and short-term changes attributable to individual events have been analyzed extensively. Increasing aerosol and cloud droplet number concentrations were associated with China’s rapid economic growth between the 1980s and 2000s (Bennartz et al., 2011). Over the past decade, however, sulfate aerosol (particularly effective CCN) and cloud droplet number concentrations have declined (McCoy et al., 2018). Recent declines in pollutants like PM2.5 and NO_2 have been driven by increasingly stringent environmental policies (Jin et al., 2016) including goals set by the 11th (2006-2010) and 12th (2011-2015) Five-Year Plans (de Foy et al., 2016b; Liu et al., 2016; van der A et al., 2017), the 2013 Air Pollution Prevention and Control Action Plan (A. Ding et al., 2019; Silver et al., 2018; Zhai et al., 2019; Zhang et al., 2019; B. Zheng et al., 2018; Y. Zheng et al., 2017), and the 2018 Three-Year Action Plan for Winning the Blue Sky Defense Battle. Ephemeral pollution decreases have also been associated with high-profile events like the 2008 Olympics and Paralympics in Beijing (Witte et al., 2009), the 2010 World Expo in Shanghai (Hao et al., 2011), and the 2014 Youth Olympic Games in Nanjing (J. Ding et al., 2015).

Research has already begun on the environmental consequences of COVID-19. Strong declines in NO_2 have been observed in Europe, China, South Korea, and the United States (Bauwens et al., 2020); however, declines in surface PM2.5 related to the early Chinese shutdown were insufficient to avoid bad haze episodes in several cities (P. Wang et al., 2020) and benefits from decreasing NO_x and PM2.5 may be offset by related increases in ozone (Shi & Brasseur, 2020). We add to this work by examining regional-scale NO_x changes alongside possible aerosol and cloud changes in the context of the 2005-2020 satellite record and drawing upon economic and emissions data to help explain the differences we observe between pollutants during China’s February 2020 shutdown.

2 Data

We analyze monthly mean pollution and cloud properties from January 2005 to April 2020 using NASA’s “A-train” satellite constellation (local overpass times ~13:30). NO_2 and SO_2 data are from the Ozone Monitoring Instrument (OMI) on Aura (Schoeberl et al., 2006) and aerosol optical depth (AOD) and liquid-phase cloud droplet effective radius (r_e) data are from the Moderate Resolution Imaging Spectroradiometer (MODIS) on Aqua (Parkinson, 2003).

The unusual stability of OMI over its now-sixteen-year lifetime, as compared to other ultraviolet imagers, makes it ideal for evaluating long-term trends (Levelt et al., 2018). We compute monthly averages using NASA’s standard daily 0.25° by 0.25° gridded products for NO_2 tropospheric column retrievals screened for cloud fractions below 30% (Krotkov et al., 2017; Krotkov et al., 2019) and planetary boundary layer (PBL) SO_2 (Krotkov et al., 2015).

Krotkov et al. (2016) contains a useful discussion of how the NO_2 and PBL SO_2 retrievals have evolved over the lifetime of the OMI/Aura mission.

For MODIS, we use standard monthly 1.0º by 1.0º gridded Collection 6.1 products for combined land and ocean AOD at 550 nm and liquid r_e retrieved using the near-infrared 2.1 μm channel and a visible channel (Hubanks et al., 2019; Platnick et al., 2017).

Monthly economic statistics from January 2005 to April 2020 are compiled from the National Bureau of Statistics of China (NBSC).

Emissions of NO_x, PM2.5, and SO_2 broken down by economic sector (IPCC, 2006) are provided by the Emissions Database for Global Atmospheric Research (EDGAR), version 5.0 (Crippa et al., 2018; Crippa et al., 2020).

We analyze the following meteorological fields from the Modern-Era Retrospective analysis for Research and Applications, Version 2 (MERRA-2): 2-m air temperature, 700 hPa potential temperature, surface pressure, and 10-m winds (Gelaro et al., 2017). Lower tropospheric stability ($\Delta\theta$) is calculated as the difference between the potential temperature at 700 hPa and the 2-m potential temperature.

3 Pollution Changes During the February 2020 Shutdown

3.1 Regression Model

Comparing observed pollution levels in 2020 to values from previous years or a long-term average can be misleading due to seasonal cycles (Shah et al., 2020) and trends in emissions and/or concentrations. To address these issues, we employ an ordinary least squares linear regression model (Pedregosa et al., 2011) to better estimate what monthly-mean air pollution and cloud properties should have been in the absence of any COVID-19-related perturbations:

$$Y(t,\phi,\lambda) = c_0 + c_{\mathrm{sol}}S_{\mathrm{cos}} + c_{\mathrm{sin}}S_{\mathrm{sin}} + c_{\mathrm{pre}}T_{\mathrm{pre}} + c_{\mathrm{post}}T_{\mathrm{post}} + c_{\mathrm{CNY}}H_{\mathrm{CNY}}, \qquad (1)$$

where Y is the geophysical variable of interest—ln(NO_2), AOD, or r_e—as a function of time (t, in months since January 2005) estimated independently at each grid box of latitude ϕ and longitude λ and the regressors S, T, and H are defined as follows. Each constant c and the intercept c_0 are calculated independently at each grid box. We use the natural logarithm of NO_2 rather than its absolute value (in units of molecules/cm^2) for the regression because NO_2 is generally distributed log-normally in space (de Foy et al., 2016b) and later analyses involve taking spatial averages (see next section). The model is fit based on data from January 2005 to December 2019 and is used to predict the expected values for January-April 2020.

The regressors S_{cos} and S_{sin} refer to idealized seasonal cycles, represented as two annual Fourier modes:

$$S_{\mathrm{cos}}(t) = \cos\left(2\pi\frac{m(t)-1}{12}\right); \quad (2)$$

$$S_{\sin}(t) = \sin\left(2\pi\frac{m(t)-1}{12}\right), \qquad (3)$$

where m refers to the calendar month (January = 1) at time t.

Next, we define the regressors T_{pre} and T_{post} as the trend in terms of months preceding or following January 2013, respectively. January 2013 was chosen as the "turning point" due to the severe haze events that occurred early that year (Huang et al., 2014; G. J. Zheng et al., 2015) that contributed to the creation of the ambitious Air Pollution Prevention and Control Action Plan in September 2013 (Jin et al., 2016).

Finally, the regressor H_{CNY} refers to whether or not the Chinese New Year holiday and related festivities (Jiang et al., 2015; Tan et al., 2009) occurred during time t. When Chinese Lunar New Year begins in February, H_{CNY} for that month is assigned a value of 1. When the holiday begins in late January with festivities lasting into early February, H_{CNY} is assigned a value of 0.5 for both months. H_{CNY} is set to zero for all other times.

Supporting information Figure S1 shows the value of each regressor as a function of time; Figure S2 shows maps of the coefficient of determination (R^2), root-mean-square (RMS) error (ϵ_{RMS}), and number of valid samples used to fit the regression (N); and Figures S3-5 show maps of the intercept and regression coefficients for ln(NO_2), AOD, and r_e, respectively.

3.2 Results

Maps of the observed (retrieved) and expected (regression) values of NO_2, AOD, and r_e for February 2020, along with the difference between the observations and expected values, are shown in Figure 2. (NO_2 values are converted into their absolute values for the sake of presentation.) There is a readily apparent decline in NO_2, in some places rivaling the magnitude of the total tropospheric column, consistent with the results of Bauwens et al. (2020). However, there are no consistent differences in either the column aerosol loading or cloud microphysics. Furthermore, regions with the largest discrepancies in the cloud and aerosol fields tend to be those with the lowest explained variance and highest RMS errors (Figure S2). The lack of AOD decline is in apparent conflict with the results of Shi & Brasseur (2020), although it should be noted that the quantities of interest (regional-scale column aerosol loading here, surface PM2.5 at specific stations in that study) are different.

To look at the differences between the observed and estimated values in greater historical perspective, we average the observed and estimated ln(NO_2) and AOD values over a region (20-42ºN, 108-125ºE) encompassing the eastern provinces of the People's Republic of China, Hong Kong, and Taiwan. We average r_e over a region (23-35ºN, 122-130ºE) in the East China Sea in which previous studies have examined aerosol-related cloud microphysical trends (Bennartz et al., 2011; McCoy et al., 2018). Results are displayed in Figure 3, with the RMS error in this case calculated using the differences between the spatially averaged observed and expected values from January 2005 to December 2019. Like the PMI indices, ln(NO_2) shows a pronounced and unprecedented decline in February 2020 followed by a rapid recovery. AOD and r_e values during 2020 are not perceptibly distinct from the 2005-2019 record.

Sulfate aerosols, which can form via the oxidation of SO_2 in the atmosphere, are a major source of cloud condensation nuclei. SO_2 in the planetary boundary layer as retrieved by OMI is noisier than the tropospheric column NO_2 retrievals (and thus best suited to analysis of dense plumes) and can be affected by factors like elevated volcanic sulfur plumes, although previous analyses have successfully analyzed regional-scale trends to gain insight into long-term pollution changes (Krotkov et al., 2016; McCoy et al., 2018). Supporting information Figure S6 shows PBL SO_2 averaged over eastern Asia with major Northern Hemisphere volcanic eruptions excluded. SO_2 levels in February 2020 are in line with the decreasing trend since 2013 and are slightly above the previous year's values, consistent with the minimal change in cloud and aerosol properties observed by MODIS.

Meteorology can also be an important driver of changes in pollution concentrations (de Foy et al., 2016b; P. Wang et al., 2020; Zhai et al., 2019; Zhang et al., 2019). Supporting information Figure S7 shows anomalies in 2-m air temperature (warmer temperatures tend to decrease NO_x concentrations but could increase PM2.5 due to enhanced secondary aerosol production), lower tropospheric stability (stronger inversions can trap pollution near the surface), surface pressure (more frequent passage of cold fronts tends to reduce pollution concentrations), and 10-m winds from MERRA-2 for February 2020. Surface temperatures were relatively warm, which may have contributed to the observed NO_2 decline and moderated AOD changes. Overall, the February 2020 meteorology fields did not depart substantially from mean 2005-2019 conditions.

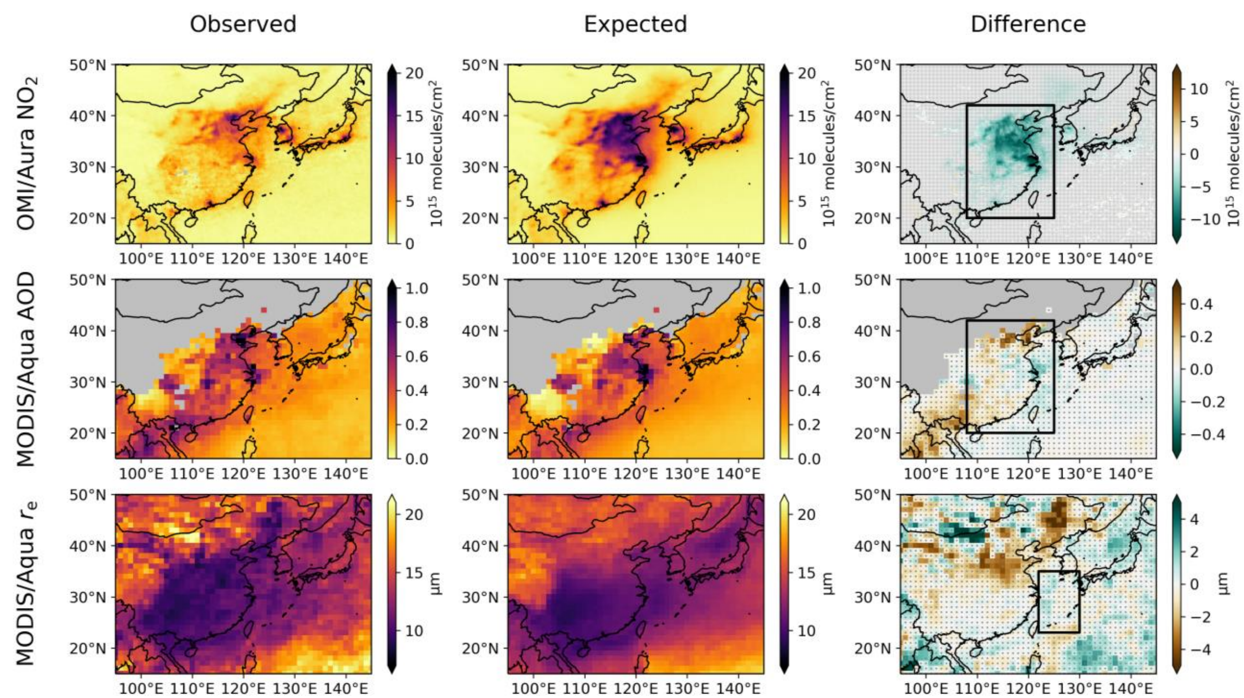

Figure 2. Change in pollution over China for February 2020. Observed values (left), estimated values (center), and their difference (right) are shown for NO_2 (top) AOD (middle), and r_e (bottom). Shading is such that lighter (left and center) and greener (right) colors align with what would be expected for decreasing pollution. Areas without valid data are shaded in gray. Gray stippling indicates absolute differences below $2\epsilon_{\mathrm{RMS}}$. Black boxes in the rightmost column indicate areas used for the averages in Figure 3.

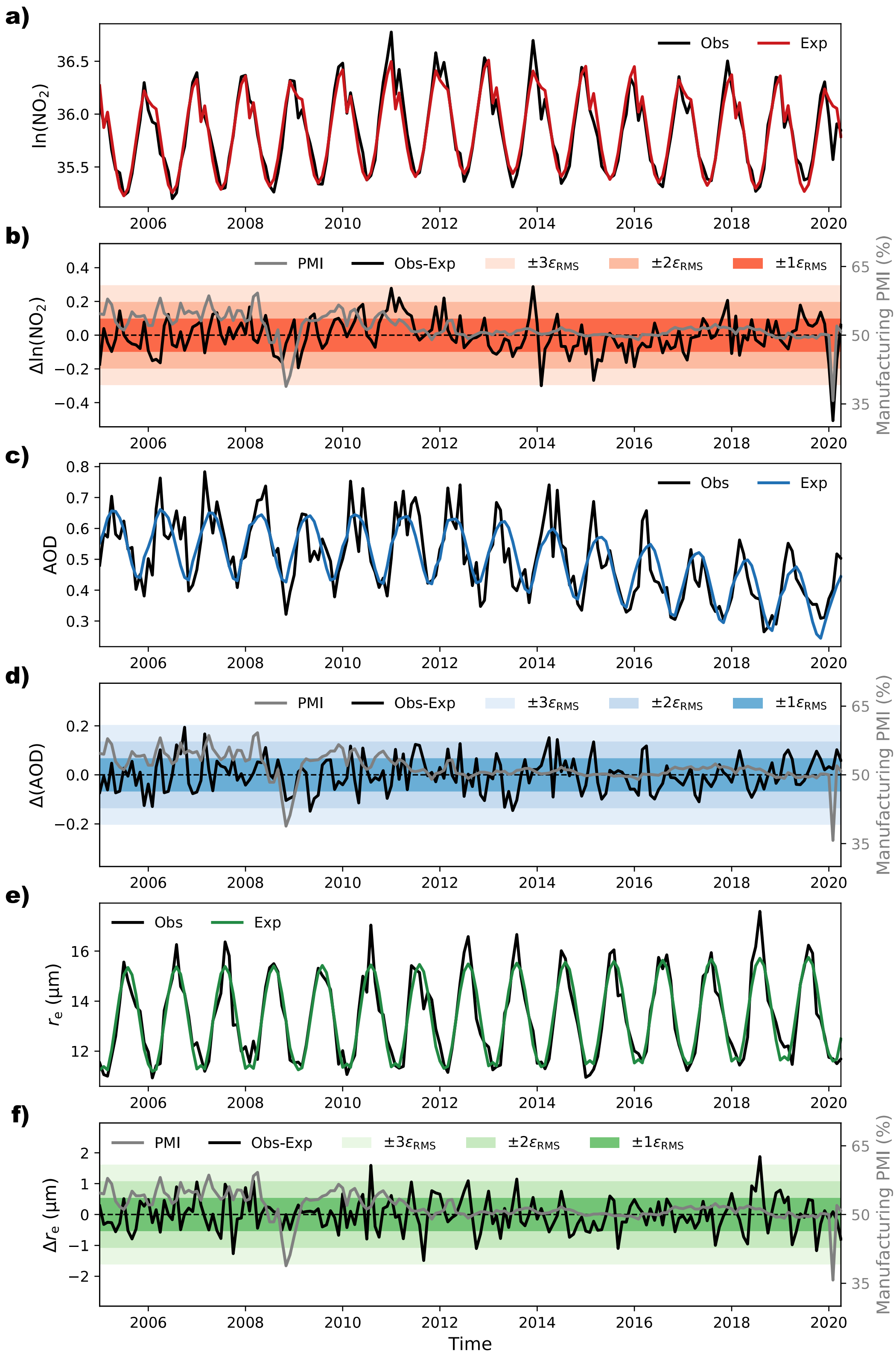

Figure 3. Time series of observed (Obs) and expected (Exp) values and their differences for **a-b)** $\ln(NO_2)$, **c-d)** AOD, and **e-f)** r_e, as averaged over the boxes in Figure 2. Manufacturing PMI is shown for reference.

4 Differential Economic and Emissions Impact of the February 2020 Shutdown by Sector

One explanation for the different NO_x and aerosol responses is that certain economic sectors which disproportionately contribute emissions of one or the other pollutant may have been impacted more or less severely by the coronavirus-induced shutdown. Figure 4 shows a sampling of records from 2005-2020 for a variety of economic sub-sectors tracked by the NBSC, including: passenger and freight transportation, iron and steel production, energy generation, and several miscellaneous industries spanning a range of products and activities. It is clear that passenger transportation, in particular, was devastated by the shutdown, whereas power generation (down ~10%, similar to 2008-2009) and heavy industries like steel production (slightly up) were comparatively unaffected, with the remainder of the economy somewhere in between. Different reporting metrics were chosen based on data quality and availability. For a more directly comparable (but temporally limited) perspective, Figure S8 shows the percentage change in accumulated production through March between 2020 and 2019 for each economic sub-sector shown in Figure 4.

Anthropogenic emissions of NO_x (E_{NO_x}), PM2.5 ($E_{PM2.5}$), and SO_2 (E_{SO_2}) in kg/m^2/s for the year 2015 from EDGAR are combined to create aggregate “transportation” and “industry and power” sectors, with the remainder lumped into an “other” category primarily consisting of agriculture and waste management. (See supporting information Tables S1-3 for the specific breakdown of the transportation, industry and power, and “other” sectors, respectively, by IPCC 2006 code.) Figure 5 shows maps of the contributions of the three pollutants by economic sector. It is clear that transportation is a major source of NO_x pollution, comparable to the industry and power sectors, whereas the industry and power sectors dominate emissions of PM2.5 and SO_2 (sulfate aerosol precursor). Given that decreases in NO_x, PM2.5, and SO_2 since 2015 have been driven primarily by regulations targeting the industrial sector (Zhang et al., 2019), it is likely that the transportation sectors made up an even greater share of total NO_x emissions in 2020 than in 2015.

Supporting information Tables S1-3 provide values for the sum of annual emissions in 2015 over the highlighted box in Figure 5 for each sector grouping. The transportation sector accounts for 26.2% of all NO_x emissions but only 4.7% of PM2.5 and 3.6% of SO_2 emissions (Table S1) while the industry and power sectors account for 72.3% of NO_x, 92.8% of PM2.5, and 95.1% of SO_2 emissions (Table S2). A steep decline passenger transportation and comparatively muted response in power generation and heavy industry thus could reasonably lead to a precipitous decline in NO_2 but little noticeable change above background variability in aerosol concentrations and SO_2.

There also exist natural sources of aerosol particles (such as sea spray and dust) and NO_x (lightning, wildfires, and soils). However, NO_x production via lightning and biomass burning is unlikely to contribute a substantial fraction of the total in China during the winter, so it is possible that a strong decline in anthropogenic NO_x emissions would be readily observable whereas a more moderate decline in anthropogenic particulate emissions (without any concomitant changes in natural sources) may not be easily detected. As a further complication, non-linear chemical interactions could result in either increasing or decreasing PM2.5 concentrations as a response to a NO_x decline depending on its magnitude and background concentrations (Zhao et al., 2017), making it plausible that, at least in some locations, increases in secondary aerosol production due to the NO_x decline could have offset reductions in primary sources.

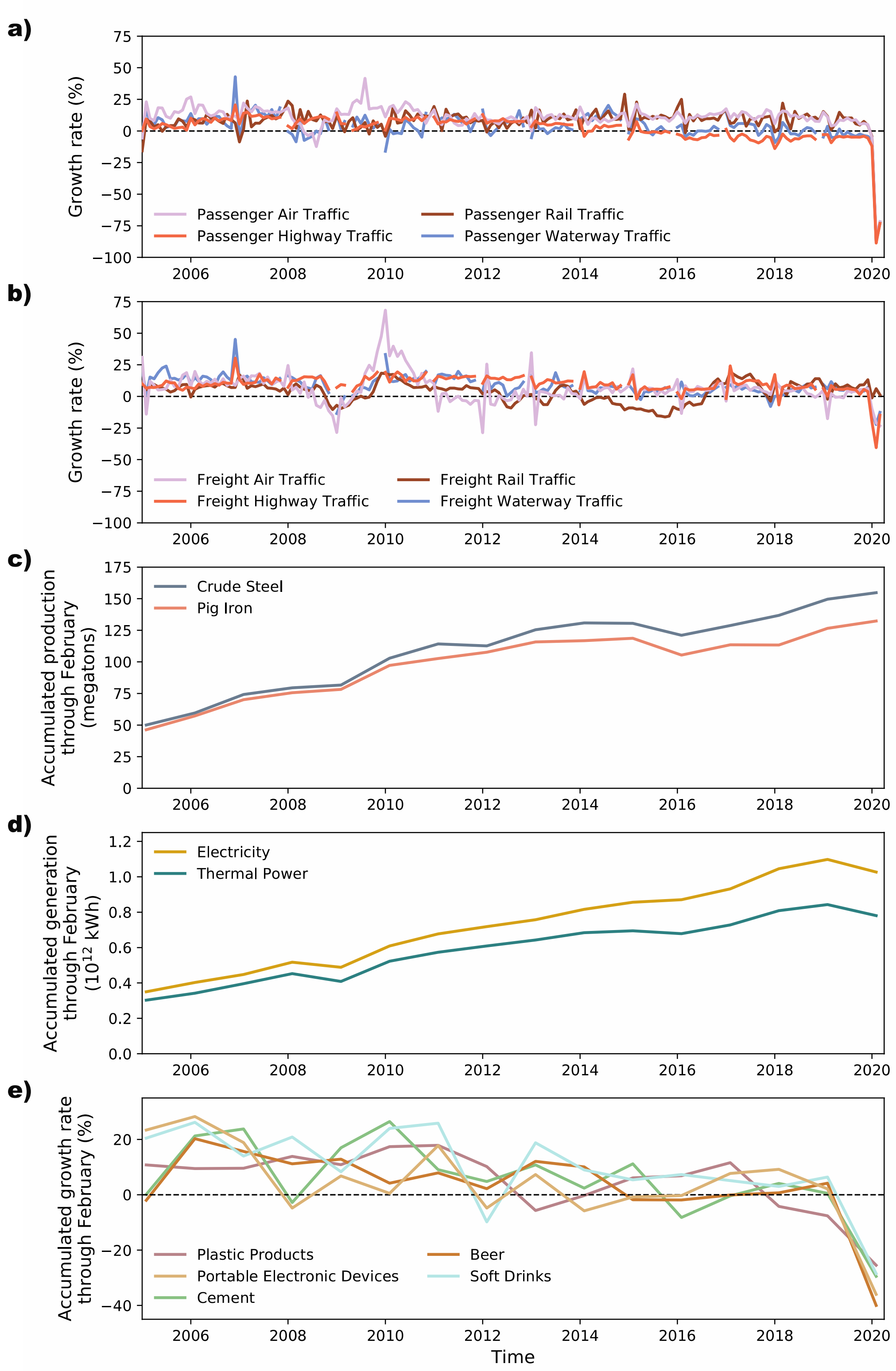

Figure 4. Time series of economic indicators. Changes in **a)** passenger and **b)** freight traffic are indicated by the growth rate (compared to the previous year) for each month between January 2005 and March 2020. **c)** Crude steel and pig iron production and **d)** power generation are indicated by the accumulated growth through February. **e)** Changes in various other industries as indicated by the growth rate (compared to the previous year) in accumulated production through February.

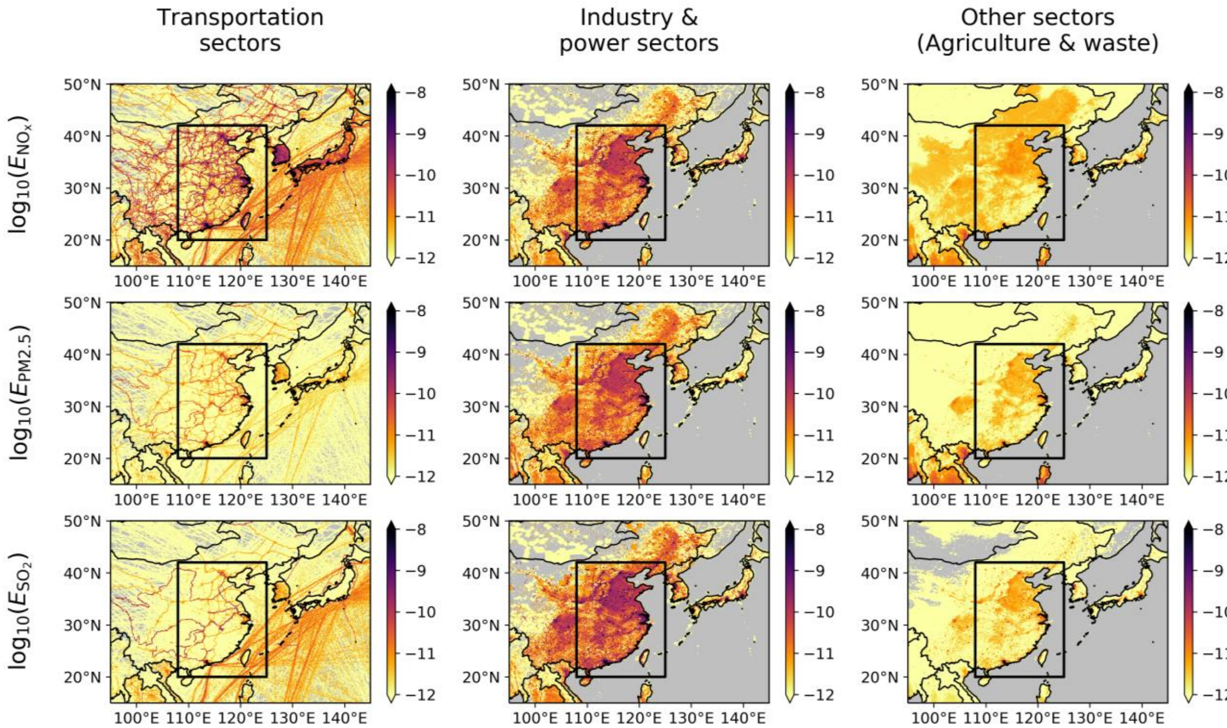

Figure 5. Emissions of major pollutants over China for 2015 from EDGAR. Values for transportation (left), industry and power (center), and other sectors (right) are shown for NO_x (top), PM2.5 (middle), and SO_2 (bottom). Areas with no recorded emissions are shaded in gray. Black boxes indicate the area used in Tables S1-3.

5 Conclusions

Despite unprecedented declines in economic activity and NO_x emissions during the February 2020 coronavirus shutdown in China, we find no detectable perturbation in aerosol and related cloud properties. The severe curtailment of passenger transportation (a disproportionate NO_x source) but comparatively muted changes in power generation and heavy industry (disproportionate PM2.5 and SO_2 sources) help explain this discrepancy, with meteorology and non-linear chemical interactions perhaps playing a supporting role.

Although no clear aerosol or cloud changes were observed in this study, longer-term changes remain possible as global economies adjust more fully to the pandemic’s effects. Medium-term environmental changes were detected as a result of the Great Recession in Europe and the United States (Castellanos & Boersma, 2012; de Foy et al., 2016a; Squizzato et al., 2018).

Further study of the environmental consequences of COVID-19 is warranted, not least because potential links between long-term and short-term air quality and vulnerability to the disease remain unresolved (Contini & Costabile, 2020). There is some evidence that short-term exposure to air pollution increased the case fatality rate of the 2002-2003 Severe Acute Respiratory Syndrome (SARS) outbreak in several Chinese cities (Cui et al., 2003), which raises the possibility of feedbacks between containment measures that happen to reduce pollution and population-level resilience. Additionally, dramatically reduced transportation sector emissions without similar changes in other sectors could represent a plausible future emissions mix if widespread electrification of transportation is adopted but other sectors do not adopt similar pollution mitigation measures.

Data Availability Statements

OMI/Aura and MODIS/Aqua Level 3 gridded data and MERRA-2 meteorological reanalysis data are publicly available from NASA's Goddard Earth Sciences Data and Information Services Center (https://disc.gsfc.nasa.gov/). Various economic statistics from the People's Republic of China are publicly available from the National Bureau of Statistics of China (http://www.stats.gov.cn/english/). EDGAR's annual sector-specific gridmaps are publicly available from the European Commission's Joint Research Center (https://edgar.jrc.ec.europa.eu/overview.php?v=50_AP; https://data.europa.eu/doi/10.2904/JRC_DATASET_EDGAR).

Acknowledgments

M. S. D. was supported by NASA Headquarters under the NASA Earth and Space Science Fellowship Program, grant NNX-80NSSC17K0404. We thank Kyle Armour, Fiona Lo, Daniel McCoy, Joel Thornton, and Casey Wall for helpful comments and discussion.

References

Ackerman, A. S., Kirkpatrick, M. P., Stevens, D. E., & Toon, O. B. (2004). The impact of humidity above stratiform clouds on indirect aerosol climate forcing. *Nature*, *432*, 1014. http://dx.doi.org/10.1038/nature03174

Albrecht, B. A. (1989). Aerosols, Cloud Microphysics, and Fractional Cloudiness. *Science*, *245*, 1227-1230.

Atkinson, R. W., Butland, B. K., Anderson, H. R., & Maynard, R. L. (2018). Long-term Concentrations of Nitrogen Dioxide and Mortality: A Meta-analysis of Cohort Studies. *Epidemiology*, *29*(4), 460-472. https://www.ncbi.nlm.nih.gov/pubmed/29746370

Bauwens, M., Compernolle, S., Stavrakou, T., Müller, J. F., Gent, J., Eskes, H., et al. (2020). Impact of coronavirus outbreak on NO2 pollution assessed using TROPOMI and OMI observations. *Geophysical Research Letters*.

Bennartz, R., Fan, J., Rausch, J., Leung, L. R., & Heidinger, A. K. (2011). Pollution from China increases cloud droplet number, suppresses rain over the East China Sea. *Geophysical Research Letters*, *38*(9), L09704.

Burnett, R., Chen, H., Szyszkowicz, M., Fann, N., Hubbell, B., Pope, C. A., 3rd, et al. (2018). Global estimates of mortality associated with long-term exposure to outdoor fine particulate matter. *Proceedings of the National Academy of Sciences*, *115*(38), 9592-9597. https://www.ncbi.nlm.nih.gov/pubmed/30181279

Castellanos, P., & Boersma, K. F. (2012). Reductions in nitrogen oxides over Europe driven by environmental policy and economic recession. *Scientific Reports*, *2*, 265. https://www.ncbi.nlm.nih.gov/pubmed/22355777

Contini, D., & Costabile, F. (2020). Does Air Pollution Influence COVID-19 Outbreaks? *Atmosphere*, *11*(4).

Crippa, M., Guizzardi, D., Muntean, M., Schaaf, E., Dentener, F., van Aardenne, J. A., et al. (2018). Gridded emissions of air pollutants for the period 1970–2012 within EDGAR v4.3.2. *Earth System Science Data*, *10*(4), 1987-2013.

Crippa, M., Solazzo, E., Huang, G., Guizzardi, D., Koffi, E., Muntean, M., et al. (2020). High resolution temporal profiles in the Emissions Database for Global Atmospheric Research. *Scientific Data*, *7*(1), 121. https://www.ncbi.nlm.nih.gov/pubmed/32303685

Cui, Y., Zhang, Z.-F., Froines, J., Zhao, J., Wang, H., Yu, S.-Z., & Detels, R. (2003). Air pollution and case fatality of SARS in the People's Republic of China: an ecologic study. *Environmental Health*, *2*(1), 15. https://doi.org/10.1186/1476-069X-2-15

de Foy, B., Lu, Z., & Streets, D. G. (2016a). Impacts of control strategies, the Great Recession and weekday variations on NO2 columns above North American cities. *Atmospheric Environment*, *138*, 74-86.

de Foy, B., Lu, Z., & Streets, D. G. (2016b). Satellite NO2 retrievals suggest China has exceeded its NOx reduction goals from the twelfth Five-Year Plan. *Scientific Reports*, *6*, 35912. https://www.ncbi.nlm.nih.gov/pubmed/27786278

Ding, A., Huang, X., Nie, W., Chi, X., Xu, Z., Zheng, L., et al. (2019). Significant reduction of PM2.5 in eastern China due to regional-scale emission control: evidence from SORPES in 2011–2018. *Atmospheric Chemistry and Physics*, *19*(18), 11791-11801.

Ding, J., van der A, R. J., Mijling, B., Levelt, P. F., & Hao, N. (2015). NOx emission estimates during the 2014 Youth Olympic Games in Nanjing. *Atmospheric Chemistry and Physics*, *15*(16), 9399-9412.

Gelaro, R., McCarty, W., Suárez, M. J., Todling, R., Molod, A., Takacs, L., et al. (2017). The Modern-Era Retrospective Analysis for Research and Applications, Version 2 (MERRA-2). *Journal of Climate*, *30*(14), 5419-5454.

Gryspeerdt, E., Quaas, J., & Bellouin, N. (2016). Constraining the aerosol influence on cloud fraction. *Journal of Geophysical Research: Atmospheres*, *121*(7), 3566-3583.

Hao, N., Valks, P., Loyola, D., Cheng, Y. F., & Zimmer, W. (2011). Space-based measurements of air quality during the World Expo 2010 in Shanghai. *Environmental Research Letters*, *6*(4).

Harris, E. S. (1991). Tracking the Economy with the Purchasing Managers' Index. *Federal Reserve Bank of New York Quarterly Review*, *Autumn*, 61-69.

Huang, R. J., Zhang, Y., Bozzetti, C., Ho, K. F., Cao, J. J., Han, Y., et al. (2014). High secondary aerosol contribution to particulate pollution during haze events in China. *Nature*, *514*(7521), 218-222. https://www.ncbi.nlm.nih.gov/pubmed/25231863

Hubanks, P. A., Platnick, S., King, M. D., & Ridgway, W. (2019). MODIS Atmosphere L3 Gridded Product Algorithm Theoretical Basis Document (ATBD) & Users Guide. https://modis-atmosphere.gsfc.nasa.gov/sites/default/files/ModAtmo/L3_ATBD_C6_C61_2019_02_20.pdf

IPCC. (2006). 2006 IPCC Guidelines for National Greenhouse Gas Inventories. In Eggleston H.S., Buendia L., Miwa K., N. T., & T. K. (Eds.), *Prepared by the National*

Greenhouse Gas Inventories Programme. Japan: IGES.

Jiang, Q., Sun, Y. L., Wang, Z., & Yin, Y. (2015). Aerosol composition and sources during the Chinese Spring Festival: fireworks, secondary aerosol, and holiday effects. *Atmospheric Chemistry and Physics, 15*(11), 6023-6034.

Jin, Y., Andersson, H., & Zhang, S. (2016). Air Pollution Control Policies in China: A Retrospective and Prospects. *International Journal of Environmental Research and Public Health, 13*(12). https://www.ncbi.nlm.nih.gov/pubmed/27941665

Krotkov, N. A., Lamsal, L. N., Celarier, E. A., Swartz, W. H., Marchenko, S. V., Bucsela, E. J., et al. (2017). The version 3 OMI NO2 standard product. *Atmospheric Measurement Techniques, 10*(9), 3133-3149.

Krotkov, N. A., Lamsal, L. N., Marchenko, S. V., Celarier, E. A., J.Bucsela, E., Swartz, W. H., et al. (2019). OMI/Aura NO2 Cloud-Screened Total and Tropospheric Column L3 Global Gridded 0.25 degree x 0.25 degree V3, NASA Goddard Space Flight Center, Goddard Earth Sciences Data and Information Services Center (GES DISC), Accessed: May 1, 2020.

Krotkov, N. A., Li, C., & Leonard, P. (2015). OMI/Aura Sulfur Dioxide (SO2) Total Column L3 1 day Best Pixel in 0.25 degree x 0.25 degree V3, Greenbelt, MD, USA, Goddard Earth Sciences Data and Information Services Center (GES DISC), Accessed: May 1, 2020.

Krotkov, N. A., McLinden, C. A., Li, C., Lamsal, L. N., Celarier, E. A., Marchenko, S. V., et al. (2016). Aura OMI observations of regional SO2 and NO2 pollution changes from 2005 to 2015. *Atmospheric Chemistry and Physics, 16*(7), 4605-4629.

Levelt, P. F., Joiner, J., Tamminen, J., Veefkind, J. P., Bhartia, P. K., Stein Zweers, D. C., et al. (2018). The Ozone Monitoring Instrument: overview of 14 years in space. *Atmospheric Chemistry and Physics, 18*(8), 5699-5745.

Liu, F., Zhang, Q., van der A, R. J., Zheng, B., Tong, D., Yan, L., et al. (2016). Recent reduction in NOx emissions over China: synthesis of satellite observations and emission inventories. *Environmental Research Letters, 11*(11).

Maier, B. F., & Brockmann, D. (2020). Effective containment explains subexponential growth in recent confirmed COVID-19 cases in China. *Science, 368*(6492), 742-746. https://science.sciencemag.org/content/sci/368/6492/742.full.pdf

Malavelle, F. F., Haywood, J. M., Jones, A., Gettelman, A., Clarisse, L., Bauduin, S., et al. (2017). Strong constraints on aerosol-cloud interactions from volcanic eruptions. *Nature, 546*(7659), 485-491. https://www.ncbi.nlm.nih.gov/pubmed/28640263

McCoy, D. T., Bender, F. A. M., Grosvenor, D. P., Mohrmann, J. K., Hartmann, D. L., Wood, R., & Field, P. R. (2018). Predicting decadal trends in cloud droplet number concentration using reanalysis and satellite data. *Atmospheric Chemistry and Physics, 18*(3), 2035-2047.

Myhre, G., Shindell, D., Bréon, F.-M., Collins, W., Fuglestvedt, J., Huang, J., et al. (2013). Anthropogenic and Natural Radiative Forcing. In T. F. Stocker, D. Qin, G.-K. Plattner, M. Tignor, S. K. Allen, J. Boschung, A. Nauels, Y. Xia, V. Bex, & P. M. Midgley (Eds.), *Climate Change 2013: The Physical Science Basis. Contribution of Working Group I to the Fifth Assessment Report of the Intergovernmental Panel on Climate Change*. Cambridge, United Kingdom and New York, NY, USA: Cambridge University Press.

Parkinson, C. L. (2003). Aqua: an earth-observing satellite mission to examine water and other climate variables. *IEEE Transactions on Geoscience and Remote Sensing, 41*(2), 173-183.

Pedregosa, F., Varoquaux, G., Gramfort, A., Michel, V., Thirion, B., Grisel, O., et al. (2011). Scikit-learn: Machine Learning in Python. *Journal of Machine Learning Research, 12*, 2825-2830.

Platnick, S., Meyer, K. G., King, M. D., Wind, G., Amarasinghe, N., Marchant, B., et al. (2017). The MODIS cloud optical and microphysical products: Collection 6 updates and examples from Terra and Aqua. *IEEE Transactions on Geoscience and Remote Sensing, 55*(1), 502-525. https://www.ncbi.nlm.nih.gov/pubmed/29657349

Schoeberl, M. R., Douglass, A. R., Hilsenrath, E., Bhartia, P. K., Beer, R., Waters, J. W., et al. (2006). Overview of the EOS aura mission. *IEEE Transactions on Geoscience and Remote Sensing, 44*(5), 1066-1074.

Shah, V., Jacob, D. J., Li, K., Silvern, R. F., Zhai, S., Liu, M., et al. (2020). Effect of changing NOx; lifetime on the seasonality and long-term trends of satellite-observed tropospheric NO₂ columns over China. *Atmospheric Chemistry and Physics, 20*(3), 1483-1495.

Shi, X., & Brasseur, G. P. (2020). The Response in Air Quality to the Reduction of Chinese Economic Activities during the COVID-19 Outbreak. *Geophysical Research Letters*.

Silver, B., Reddington, C. L., Arnold, S. R., & Spracklen, D. V. (2018). Substantial changes in air pollution across China during 2015–2017. *Environmental Research Letters, 13*(11).

Squizzato, S., Masiol, M., Rich, D. Q., & Hopke, P. K. (2018). PM2.5 and gaseous pollutants in New York State during 2005–2016: Spatial variability, temporal trends, and economic influences. *Atmospheric Environment, 183*, 209-224.

Stevens, B., & Feingold, G. (2009). Untangling aerosol effects on clouds and precipitation in a buffered system. *Nature, 461*(7264), 607-613.

Storelvmo, T. (2017). Aerosol Effects on Climate via Mixed-Phase and Ice Clouds. *Annual Review of Earth and Planetary Sciences, 45*(1), 199-222. https://www.annualreviews.org/doi/abs/10.1146/annurev-earth-060115-012240

Tan, P.-H., Chou, C., Liang, J.-Y., Chou, C. C. K., & Shiu, C.-J. (2009). Air pollution “holiday effect” resulting from the Chinese New Year. *Atmospheric Environment, 43*(13), 2114-2124.

Tian, H., Liu, Y., Li, Y., Wu, C.-H., Chen, B., Kraemer, M. U. G., et al. (2020). An investigation of transmission control measures during the first 50 days of the COVID-19 epidemic in China. *Science*, eabb6105. https://science.sciencemag.org/content/sci/early/2020/03/30/science.abb6105.full.pdf

Toll, V., Christensen, M., Quaas, J., & Bellouin, N. (2019). Weak average liquid-cloud-water response to anthropogenic aerosols. *Nature, 572*(7767), 51-55.

Twomey, S. (1977). The Influence of Pollution on the Shortwave Albedo of Clouds. *Journal of the Atmospheric Sciences, 34*(7), 1149-1152. http://journals.ametsoc.org/doi/abs/10.1175/1520-0469%281977%29034%3C1149%3ATIOPOT%3E2.0.CO%3B2

van der A, R. J., Mijling, B., Ding, J., Koukouli, M. E., Liu, F., Li, Q., et al. (2017). Cleaning up the air: effectiveness of air quality policy for SO2 and NOx emissions in China. *Atmospheric Chemistry and Physics, 17*(3), 1775-1789.

Wang, C., Horby, P. W., Hayden, F. G., & Gao, G. F. (2020). A novel coronavirus outbreak of global health concern. *The Lancet, 395*(10223), 470-473.

Wang, P., Chen, K., Zhu, S., Wang, P., & Zhang, H. (2020). Severe air pollution events not avoided by reduced anthropogenic activities during COVID-19 outbreak. *Resources,* *Conservation, & Recycling, 158*, 104814. https://www.ncbi.nlm.nih.gov/pubmed/32300261

Witte, J. C., Schoeberl, M. R., Douglass, A. R., Gleason, J. F., Krotkov, N. A., Gille, J. C., et al. (2009). Satellite observations of changes in air quality during the 2008 Beijing Olympics and Paralympics. *Geophysical Research Letters, 36*(17).

Zhai, S., Jacob, D. J., Wang, X., Shen, L., Li, K., Zhang, Y., et al. (2019). Fine particulate matter (PM2.5) trends in China, 2013–2018: separating contributions from anthropogenic emissions and meteorology. *Atmospheric Chemistry and Physics, 19*(16), 11031-11041.

Zhang, Q., Zheng, Y., Tong, D., Shao, M., Wang, S., Zhang, Y., et al. (2019). Drivers of improved PM2.5 air quality in China from 2013 to 2017. *Proceedings of the National Academy of Sciences, 116*(49), 24463-24469.

Zhao, B., Wu, W., Wang, S., Xing, J., Chang, X., Liou, K.-N., et al. (2017). A modeling study of the nonlinear response of fine particles to air pollutant emissions in the Beijing–Tianjin–Hebei region. *Atmospheric Chemistry and Physics, 17*(19), 12031-12050.

Zheng, B., Tong, D., Li, M., Liu, F., Hong, C., Geng, G., et al. (2018). Trends in China's anthropogenic emissions since 2010 as the consequence of clean air actions. *Atmospheric Chemistry and Physics, 18*(19), 14095-14111.

Zheng, G. J., Duan, F. K., Su, H., Ma, Y. L., Cheng, Y., Zheng, B., et al. (2015). Exploring the severe winter haze in Beijing: the impact of synoptic weather, regional transport and heterogeneous reactions. *Atmospheric Chemistry and Physics, 15*(6), 2969-2983.

Zheng, Y., Xue, T., Zhang, Q., Geng, G., Tong, D., Li, X., & He, K. (2017). Air quality improvements and health benefits from China’s clean air action since 2013. *Environmental Research Letters, 12*(11).